



## Review of accelerator gadgets for art and archaeology

T. Calligaro<sup>\*</sup>, J.-C. Dran, J. Salomon, Ph. Walter

*Centre de recherche et de restauration des musées de France, CNRS UMR 171, Palais du Louvre-Porte des Lions, 75001 Paris, France*

Received 21 October 2003; received in revised form 1 April 2004

### Abstract

For 30 years analytical methods based on ion beams have been progressively adapted to art and archaeological issues. By allowing the analysis of artefacts in a non-invasive and non-destructive way, the external beam represents the cornerstone of this evolution. In order to reach in air specifications usually obtained under vacuum, improvements in various directions have been necessary. A large panel of gadgets and experimental arrangements have been designed such as a multi-detector set-up operating in helium atmosphere to extend the range of measured elements, a nuclear microprobe at atmospheric pressure for the study of microscopic details or a reliable beam monitoring system. In addition, specific procedures have been developed to characterise multi-layered samples (easel paintings, alteration layers) by varying either the beam energy or the impinging angle. To improve the sensitivity to trace elements in high-*Z* materials like metals or for analysing targets too sensitive to stand direct exposure to charged particles, a specific X-ray fluorescence set-up (PIXE-XRF) based on the production of quasi-monochromatic X-rays has been developed. Eventually, the ion beam methods usually restricted for external beams to those based on photon detection (PIXE, PIGE) have been recently extended to methods based on charged particle detection (RBS, NRA and even ERDA), opening new perspectives for determination of light elements and depth profiling. This paper makes an historical review of the adaptation of IBA methods to the study of cultural heritage.

© 2004 Elsevier B.V. All rights reserved.

*PACS:* 29.27.Ac; 34.50.Bw; 82.80.Yc

*Keywords:* Art; Archaeometry; External beam; PIXE; RBS; NRA; Nuclear microprobe

### 1. Specific constraints for the analysis of works of art and archaeological items

Due to their high artistic or historical value, the chemical characterisation of cultural heritage items

should rely on non-invasive and non-destructive methods. Under the non-invasive term we understand that any sampling or dismantling of the artefact is avoided and more generally that its integrity and its environment are preserved (for example, the object should be placed in an atmosphere compatible with its preservation and not vacuum). The non-destructive character means that the analysis does not alter nor modify in any way the investigated area. An important feature of the cultural goods lays in the extremely diverse

<sup>\*</sup> Corresponding author. Tel.: +33-1-40-205413; fax: +33-1-47-33246.

*E-mail address:* [thomas.calligaro@culture.gouv.fr](mailto:thomas.calligaro@culture.gouv.fr) (T. Calligaro).

composition and structure of their materials. To characterise an item of composition a priori unknown, the selected methods have to be panoramic, i.e. able to dose a range of elements as complete as possible, ideally covering the entire periodic table. Moreover, since composition is seldom homogeneous, these methods must possess a good spatial resolution, laterally and in-depth so as to determine, for example, the composition and the arrangement of paint layers of an easel painting.

This paper aims at showing how ion beam methods have been progressively adapted to the study of cultural heritage materials. The milestones of this development are highlighted, in answer to the issues and the specific constraints imposed by these items.

## 2. Charged particles in air: the external beam

The study of cultural heritage has benefited from the analytical qualities of ion beam analytical techniques (IBA) since their introduction, as evidenced by works in the early 1970's using PIXE in vacuum on iron-based pigments of potteries in Brookhaven [1] or using PIGE on obsidians in New Zealand [2]. During the same period, external beam lines have been designed by several laboratories among which the pioneering group in Namur [3] for the analysis of fragile samples or targets unable to stand vacuum like organic compounds or liquids. The basic principle of the external beam is to send the particle beam into the surrounding atmosphere through a few-micron thick exit window, ensuring the vacuum/air interface, and to bombard the sample placed a few millimetres downstream. Soon applied to art and archaeology, particularly in Athens [4], the external beam can be considered as the cornerstone of the adaptation of ion beam analysis to this field

since it perfectly matches the non-invasive and non-destructive character mentioned above. Let us recall the major benefits of the external beam:

- it allows the analysis of items of any size and shape
- it avoids the alteration due to vacuum (dehydration, outgassing, etc.)
- it reduces the risk of heating and beam-induced damage
- it eliminates the need of sample preparation such as the deposit of conductive coating
- it improves system efficiency by simplifying sample positioning and changing.

A detailed review of the advantages and limitations of external beams has been published by Mandò [5]. Many efforts have been made in the geometric design of the “nozzle” of the external beam set-up, to allow the analysis of most areas of complex-shaped artefacts: compact and pointed geometry, use of subminiature video camera or long-distance zoom optics. Many window types have been tested in order to find the best material combining good mechanical strength, high resistance to beam damage and low background radiation [6]. Table 1 shows the specifications of widespread windows made of metals and Kapton®, an organic polymer resistant to radiation. PIXE and PIGE remains the predominantly used methods used in air as they are less sensitive to the energy degradation and angular divergence suffered by the beam as it passes through the window and along the air path. The fragility of the foils has needed the implementation of high speed valve on the external beam lines to prevent the vacuum degradation in the facility in case of window breakdown. But the major challenge of the external beam is the design of a dose monitoring system, as direct charge integration in air is

Table 1

Specifications of some widely used exit windows: composition and thickness, energy loss  $\Delta E$ , energy straggling  $\sigma_E$  and angular straggling  $\sigma_\theta$ , beam diameter for 3-MeV protons and applicable IBA method

Material	$t$ ( $\mu\text{m}$ )	$\Delta E$ (keV)	$\sigma_E$ (keV)	$\sigma_\theta$ ( $\mu\text{m}/\text{mm}$ )	$\emptyset$ ( $\mu\text{m}$ )	IBA method
Aluminium	10	233	15.9	14	150	PIXE/PIGE
Kapton®	8	129	9.0	6	500	PIXE/PIGE
Zirconium	2	73	7.3	15	200	d-PIXE DIGE d-NRA

impracticable. To solve this problem various arrangements have been developed, based on the interaction of the beam with either a chopper [7], the exit window (PIXE, PIGE or RBS signals [8]) or the surrounding air (argon X-rays, or even iono-luminescence [9]).

### 3. Extending the range of measured elements in PIXE/PIGE mode

In the early times, PIXE experiments were mainly carried out to determine medium to high  $Z$  elements at trace level, using a single Si(Li) detector with a single 3-MeV proton irradiation, and the main constituents were supposed to be known (previously measured by other methods, e.g. SEM-EDX or XRF). To extend the range of measured elements to low  $Z$  elements ( $Z < 20$ ) which are often the major constituents of the sample, and to make the analysis independent from any other method, a procedure based on two successive runs at low and high beam energies was used to determine all elements above sodium (e.g. 1 MeV without X-ray filter and 3 MeV with a suitable absorber). This

situation was greatly improved by the introduction of a dual-detector system with a single run at 3 MeV by the Florence group [10]. In this innovative set-up, a first Si(Li) detector flushed with helium is used to measure light elements ( $11 < Z < 30$ ) while a second one, equipped with a suitable absorber, is used for the determination of trace elements ( $Z > 20$ ). In addition to the gain in time, this set-up can be easily tuned for the analysis of a broad range of materials by optimising the sample-to-detector distances and selecting an adequate X-ray absorber. This arrangement has been further improved in Paris by the addition of a HPGe  $\gamma$ -ray detector for ultra-light elements (B, Be, Li, F), a

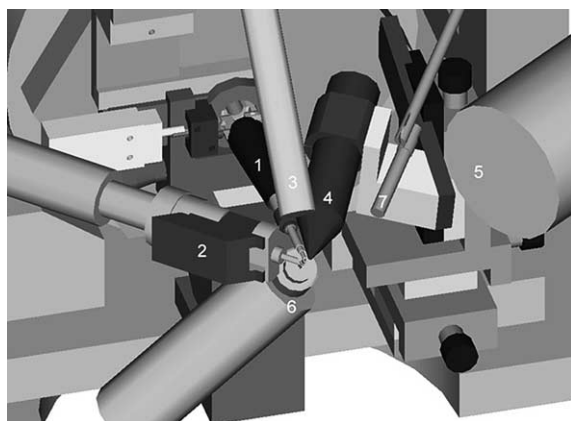


Fig. 1. External beam layout of the quadruple detector external beam set-up used to perform PIXE, PIGE and RBS with a single 3-MeV proton run. (1) Nozzle ended with the exit window. (2) Magnetic deflector for the filterless Si(Li) detector (1–15 keV range). (3) Si(Li) detector for the 5–40 keV range. (4) Charged particle detector for RBS/NRA. (5) HPGe  $\gamma$ -ray detector. (6) Peltier-cooled X-ray detector for monitoring the beam dose using the silicon PIXE signal emitted by the exit window. (7) Subminiature video camera.

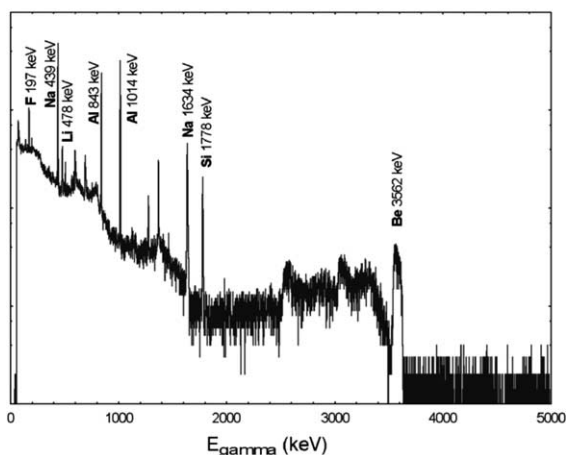
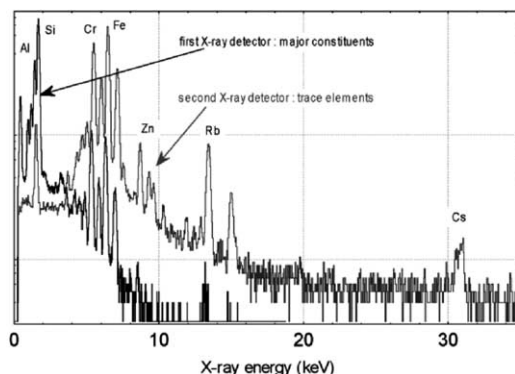


Fig. 2. PIXE and PIGE spectra of ancient emerald set on Visigoth royal crowns excavated in Guarrazar, Iberic Peninsula (8th century A.D.). In addition to the main constituents of the emerald (Be, Al, Si), the two PIXE and the PIGE spectra show various trace elements (Li, F, Na, Mg, Ca, Ti, Rb, Ni, Cu, Zn, Cs) used to infer the origin of these gemstones.

deflector against backscattered particles based on permanent magnets, a charged particle detector for RBS and a monitoring system for the beam dose [11] (Fig. 1). As an illustrating application of this multi-detector system we can mention the determination of the provenance of emeralds set on Visigothic royal crowns from the eighth century. As shown in Fig. 2, the PIXE and PIGE spectra collected in a single 3-MeV run show that the beryl crystal of formula  $\text{Be}_3\text{Al}_2(\text{SiO}_3)_6$  has incorporated in its structure various trace elements such as Na, Mg, Ca, Ti, Rb, Ni, Cu, Zn, Cs but also very light ones such as Li, F. This trace element fingerprint was used to establish that these barbarian emeralds were extracted from the Alps rather than from Egypt or Asia as it was the case for the Roman ones [12].

#### 4. Nuclear microprobe at atmospheric pressure

Whereas the diameter of the first external beams was macroscopic (of the order of a fraction of millimetre), a strong demand for a smaller spot size in air has rapidly grown. The first method employed to reduce the probe size was based on a graphite pinhole collimator. In an early attempt in 1975 a collimated beam with a 10- $\mu\text{m}$  diameter has been obtained without any exit window, simply with a differential pumping stage [13]. However, the main disadvantages of such systems, namely the low intensity and the beam halo induced by the scattering of the beam on the collimator edges could only be circumvented with the help of focusing lenses used in vacuum microprobes. The introduction of ultra-thin windows (0.1  $\mu\text{m}$ ) made of  $\text{Si}_3\text{N}_4$ , really boosted external micro-beam development, specially in reducing the achievable beam spot size [14]. Primarily designed as sample holders for TEM equipment, these windows also revealed to be extremely resistant to ion beams. By mounting such a window at the exit of a conventional microprobe set-up, the group of Paris has designed an authentic in-air nuclear microprobe exhibiting a 10- $\mu\text{m}$  diameter with protons and 30- $\mu\text{m}$  diameter with alpha beam [15]. Although these specifications are far away from the sub-micronic resolution obtained by in vacuo microprobes, they are adequate to

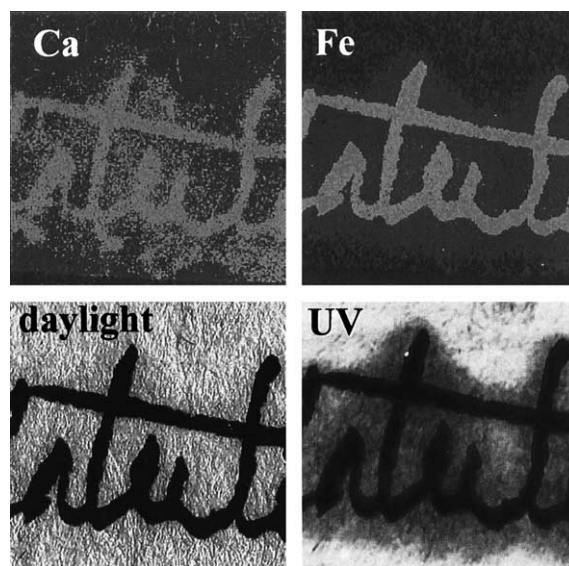


Fig. 3. Elemental maps and visual aspects under daylight and UV light of an altered manuscript showing the migration of Ca and Fe around the characters written using an iron-gall ink. The scanned area is  $10 \times 10 \text{ mm}^2$ .

carry out most of the studies concerning cultural heritage, the beam penetrating anyway the artefact material at a depth of some tens of micrometres [16]. Elemental maps can be obtained either by mechanically scanning the sample under a fixed micro-beam with stepping motors or by scanning the beam with magnetic coils. The first mode permits to scan quite large areas (up to several  $\text{cm}^2$ ) out of reach with conventional nuclear microprobes operating under vacuum, whereas the second mode, although limited by the size of the exit window ( $1 \times 1 \text{ mm}$ ), is suitable for mapping microscopic details. For example, a large area scan ( $1 \times 1 \text{ cm}$ ) was used for the study of manuscript damaged by iron-gall ink corrosion [17]. The comparison of the optical image with the Ca and Fe maps in Fig. 3 shows the smearing of the ink constituents out of the written characters.

#### 5. Elemental depth profiling: paint layers and surface alteration

Profiling methods based upon PIXE, PIGE or RBS methods with external proton beams have

been developed to characterise the layered structure or the elemental depth profile at the surface of many objects relevant to cultural heritage. External p-RBS, despite its poor discrimination for heavy elements and its departure from the Rutherford law has been used for the characterisation of multi-layers [18]. For instance, the external p-RBS spectrum in Fig. 4 illustrates the characterisation of patina of historical Japanese swords. It shows that the traditional Au/Cu alloy named *Shakudo* is covered with a patina composed mainly of copper oxide and a varnish layer. The PIXE method has also been employed for depth profiling using two approaches: varying the energy of the beam and its incident angle. The first solution makes use of the variation of the X-ray yield of a given element at different proton energies (typically 1–3 MeV with 0.5 MeV steps). Despite its

much poorer depth resolution than p-RBS, it allows to probe deeper in the material [19]. The energy of the impinging beam can be conveniently changed by inserting suitable foils between the exit window and the sample [20], at the expense of a varying spot size. The benefit of this approach is to keep constant the accelerator conditions, avoiding the tedious sample repositioning after each beam energy modification; it also simplifies the dose monitoring. A second approach for depth profiling with PIXE/PIGE is based on the change of the impinging direction of the beam, for instance from  $0^\circ$  to  $70^\circ$  by step of  $10^\circ$ . This solution is simple provided that the analysed location is kept fixed while changing the angle (eucentric rotation), and that the sample surface is smooth and flat [21]. The merits of RBS-based and PIXE-based profiling methods for the determination of the composition,

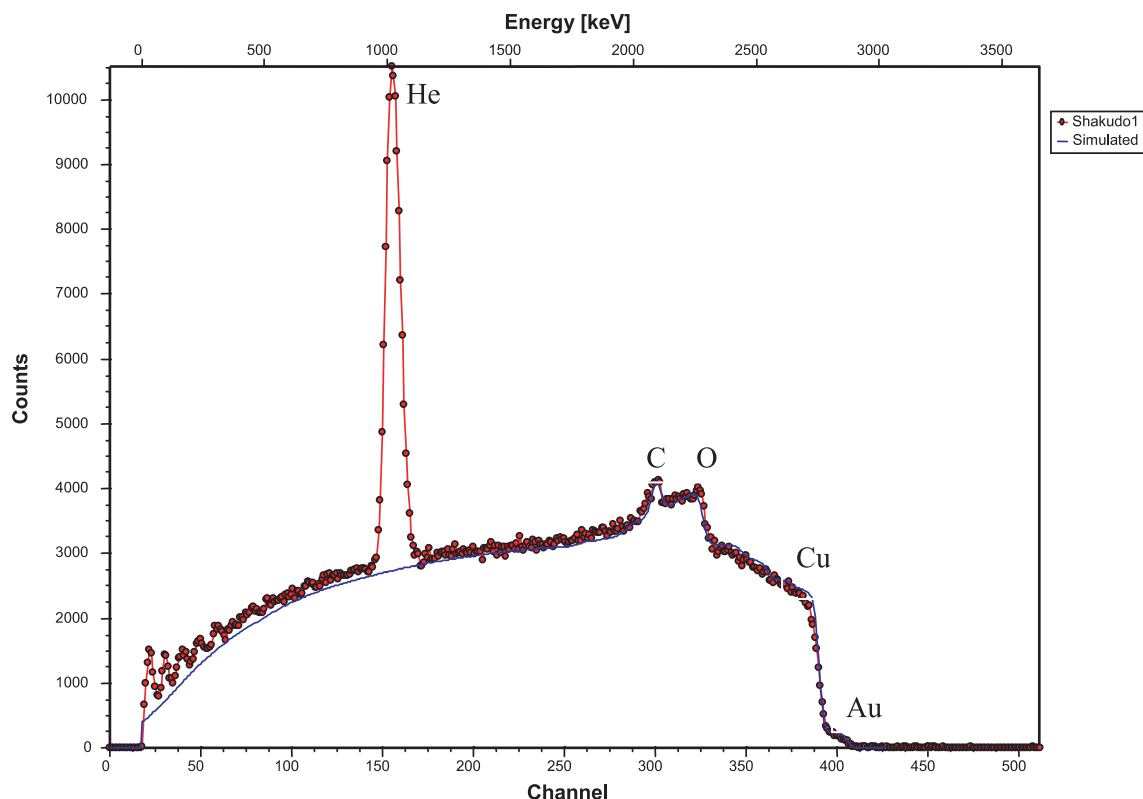


Fig. 4. RBS spectrum of the hilt of a historical Japanese sword. The hilt is made of a traditional Au/Cu alloy named *Shakudo* covered with a patina composed mainly of copper oxide and a varnish layer. The spectrum is obtained with an external 3-MeV proton beam in a helium atmosphere, producing an intense He peak which can be used for dose monitoring and energy calibration.

the ordering and the thickness of paint layers in easel paintings has been compared in the framework of a large collaboration between several laboratories [22].

## 6. Improving the limits of detection

In PIXE mode, the measurement of trace elements in materials mainly composed of high-Z

elements such as metallic alloys represents a difficult task. In order not to be obscured by the strong X-ray emission of the main constituents two solutions have been considered. The first makes use of selective filters to attenuate the matrix signals while preserving the lines of searched element [23]. This method can only be applied when the X-ray lines of the trace element lays just below the lines of the main constituents, and when a filter material which has an absorption edge between

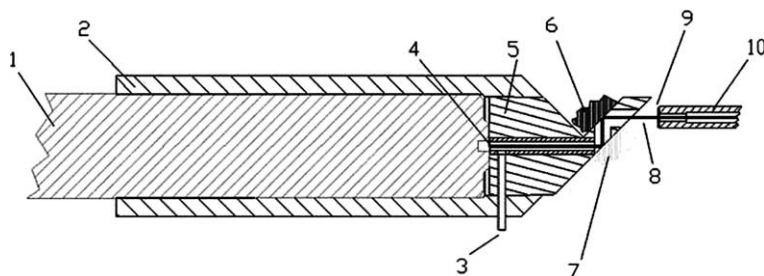


Fig. 5. PIXE-XRF layout for the in-air measurement of platinum in gold. (1) Housing of the Peltier-cooled *silicon-drift* detector for the collection of fluorescent X-rays. (2) Setup housing. (3) Helium inlet for cooling the intermediate As target. (4) Zinc absorber in front of the Si crystal. (5) Aluminium part. (6) Arsenic intermediate target. (7) Gold sample being analysed. (8) Proton beam. (9) Exit window. (10) Beam line.

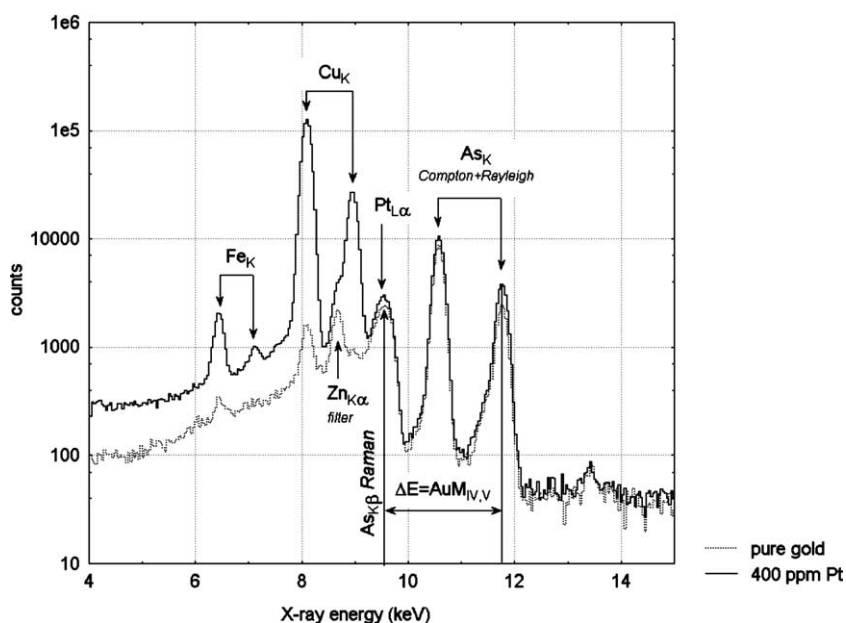


Fig. 6. PIXE-XRF spectra recorded on pure gold and a gold sample containing 400 ppm platinum. The peak rising at 9.4 keV corresponds to the overlap of the Pt signal and the Raman scattering of the As  $K\beta$ . Using this setup, the detection limit of platinum was lowered to 50 ppm, compared to 1000 ppm at best for PIXE.

these lines can be found. The second solution, introduced in the very early times, relies on a variant of X-ray fluorescence called PIXE-XRF [24]. In this technique, an intermediate target is bombarded with protons to produce a strong X-ray emission, that can in turn serve as a versatile source for X-ray fluorescence. This almost monochromatic and background-free X-ray emission can thus selectively excite the trace element of interest without exciting the major constituents of the sample [25]. Fig. 5 depicts such an external PIXE-XRF set-up and Fig. 6 shows the spectrum recorded on archaeological gold with trace amount

of platinum. With this arrangement, the limit of detection of Pt in Au reaches  $\approx 50$  ppm, 20 times lower than the 1000 ppm obtained with PIXE [26]. Another benefit of the PIXE-XRF technique is that it can be used for the XRF analysis of items prone to damage when bombarded with ion beams (e.g. organic materials such as paper, hair, skin, etc.). In this mode, PIXE-XRF has two advantages over conventional XRF methods with X-ray tubes: the excitation energy can be easily tuned by changing the intermediate target and the radiation is produced almost without any background, providing improved limits of detection.

Table 2

Beam specifications obtained with the 0.1- $\mu\text{m}$   $\text{Si}_3\text{N}_4$  exit window: energy straggling  $\sigma_E$ , beam diameter, beam intensity and applicable IBA method

Particle	$E$ (MeV)	$\sigma_E$ (keV)	$\emptyset$ ( $\mu\text{m}$ )	$I$ (nA)	IBA method
$^1\text{H}$	3	4.5	10–20	0.05–1	PIXE / PIGE / RBS
$^4\text{He}^{++}$	3	30	50–100	5	$\alpha$ -RBS
$^4\text{He}^{++}$	3	30	50–100	5	$\alpha$ -ERDA
$^2\text{H}$	2	8	10–20	10	NRA

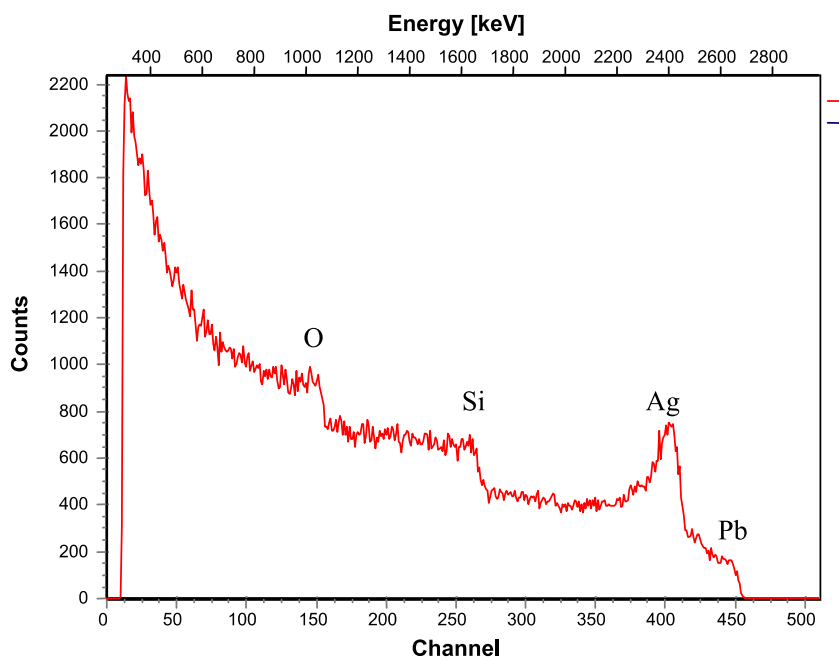


Fig. 7. RBS spectrum of a fragment of a lustred Islamic ceramic obtained with 3-MeV alpha external beam. The lustre is a lead-rich glassy layer containing silver aggregates.

## 7. Beyond protons: $\alpha$ -RBS and $\alpha$ -ERDA at atmospheric pressure

In addition to the improvement in spatial resolution used for the external microprobe, the ultra-thin  $\text{Si}_3\text{N}_4$  window allowed to implement IBA techniques based on particles heavier than protons. Table 2 gives the specifications obtained with this window, for protons, helium and deuterons beams. The extraction at atmospheric pressure of helium beams has opened the way to external  $\alpha$ -RBS in air [27], and recently  $\alpha$ -ERDA for the measurement of hydrogen [28]. These techniques can provide elemental depth profiles of high significance at the surface of art and archaeological objects, for instance to study patinas or weathering processes. Fig. 7 illustrates the profiling of Ag by  $\alpha$ -RBS in a Pb-based glaze (lustre) of an Islamic ceramic. Because energy loss of helium ions is much larger than for protons, the path of ions in the surrounding gas (air or He) must be as short as possible. This is why the external  $\alpha$ -RBS set-up makes use of two ultra-thin windows: one on the way towards the target (exit window) and one on the way to the charged particle detector (detector window), which is placed in vacuum. In external ERDA, the second window is not necessary because a thick absorber is anyhow needed in front of the charged particle detector. Besides the obvious ease of use and non-destructive character, IBA with external helium beams exhibits two advantages: external-RBS can be used in the field of experimental archaeology, for example to study in real time the transformation kinetics (oxidation or aqueous corrosion) of materials of archaeological interest [30] and in external-ERDA the hydrogen layer at the surface is reduced compared to vacuum operation.

## 8. Conclusion and prospects

The study of works of cultural heritage likely constitutes the field of application where ion beam analysis fully exhibits its unique combination of good analytical capability and non-destructive character. These features explain its quite early application to this field and the constant efforts to

improve its performance. Indeed much progress has been achieved since the first international meeting dedicated to Art and Archaeology held in 1985 in Pont-à-Mousson [29], which has emphasised the potential impact of IBA in this field. Thanks to the large panel of experimental gadgets and innovating techniques originating from this dynamics, the use of ion beams in art history and archaeology has constantly gained popularity and is acknowledged world wide, for instance through the European support to the COST G1 action (collaboration of 21 laboratories from 12 countries for the ion beam study of art and archaeological objects [31]). Many other specific developments should have been detailed in this review, such as the use of high energy beams, the design of portable systems for *on the field* IBA with radio-resources, or the combination of IBA with other non-destructive analytical methods like Raman spectrometry. Even if today external beam set-ups have reached a high level of sophistication, still some progress is needed to render accelerator methods more systematically and routinely applied to the study of our cultural heritage.

## Acknowledgements

We gratefully acknowledge the precious help of Brice Moignard for the design and machining of external beam components and Laurent Pichon for the development of the electronics, data acquisition and spectrum processing.

## References

- [1] B.M. Gordon, H.W. Kraner, J. Radioanal. Chem. 12 (1) (1972) 181.
- [2] G. Coote, N.E. Whitehead, G.J. McCallum, J. Radioanal. Chem. 12 (2) (1972) 491.
- [3] G. Deconninck, J. Radioanal. Chem. 12 (1) (1972) 157.
- [4] A.A. Katsanos, A. Xenoulis, A. Hadjiantoniou, R.W. Fink, Nucl. Instr. and Meth. 137 (1976) 119.
- [5] P.A. Mandò, Nucl. Instr. and Meth. B 85 (1994) 815.
- [6] T. Calligaro, J.-C. Dran, H. Hamon, B. Moignard, J. Salomon, Nucl. Instr. and Meth. B 136 (1998) 339.
- [7] P. Del Carmine, F. Lucarelli, P.A. Mando, A. Pecchioli, Nucl. Instr. and Meth. B 75 (1993) 480.
- [8] G. Deconninck, F. Bodart, Nucl. Instr. and Meth. 149 (1978) 609.

- [9] J.-O. Lill, Nucl. Instr. and Meth. B 150 (1999) 114.
- [10] J.D. MacArthur, P. Del Carmine, F. Lucarelli, P.A. Mandò, Nucl. Instr. and Meth. B 45 (1990) 315.
- [11] T. Calligaro, J.D. MacArthur, J. Salomon, Nucl. Instr. and Meth. B 109–110 (1996) 125.
- [12] T. Calligaro, J.-C. Dran, J. Salomon, J.-P. Poirot, Nucl. Instr. and Meth. B 161–163 (2000) 769.
- [13] L. Grodzins, P. Horowitz, J. Ryan, Science 189 (1975) 795.
- [14] H.W. Lefevre, R.M. Schofield, D.R. Ciarlo, Nucl. Instr. and Meth. B 54 (1991) 47.
- [15] T. Calligaro, J.-C. Dran, E. Ioannidou, B. Moignard, L. Pichon, J. Salomon, Nucl. Instr. and Meth. B 161–163 (2000) 328.
- [16] C.P. Swann, Nucl. Instr. and Meth. B 130 (1997) 289.
- [17] C. Remazeilles, V. Quillet, T. Calligaro, J.-C. Dran, L. Pichon, J. Salomon, Nucl. Instr. and Meth. B 181 (2001) 681.
- [18] L. Giuntini, P.A. Mandò, Nucl. Instr. and Meth. B 85 (1994) 744.
- [19] G. Demortier, S. Mathiot, B. Van Oystaeyen, Nucl. Instr. and Meth. B 49 (1990) 46.
- [20] G. Brunner, Nucl. Instr. and Meth. 166 (1979) 503.
- [21] G. Weber, D. Strivay, L. Martinot, H.P. Garnir, Nucl. Instr. and Meth. B 189 (2002) 350.
- [22] C. Neelmeijer, W. Wagner, H.P. Schramm, Nucl. Instr. and Meth. B 118 (1996) 338.
- [23] C.P. Swann, S.J. Fleming, Nucl. Instr. and Meth. B 49 (1990) 65.
- [24] Ts. Lin, Ch. Luo, J. Chou, Nucl. Instr. and Meth. 151 (1978) 439.
- [25] PIXE gadgets G. Demortier, Y. Morciaux, Nucl. Instr. and Meth. B 85 (1994) 112.
- [26] M.F. Guerra, Nucl. Instr. and Meth. B, this issue. doi:10.1016/j.nimb.2004.02.019.
- [27] E. Ioannidou, D. Bourgarit, T. Calligaro, J.-C. Dran, M. Dubus, J. Salomon, P. Walter, Nucl. Instr. and Meth. B 161–163 (2000) 730.
- [28] T. Calligaro, J. Castaing, J.-C. Dran, B. Moignard, J.-C. Pivin, G.V.R. Prasad, J. Salomon, P. Walter, Nucl. Instr. and Meth. B 181 (2001) 180.
- [29] Proceedings of the International Workshop on Ion Beam Analysis in the Arts and Archaeology Ch. Lahanier, G. Amsel, Ch. Heitz, M. Menu, H.H. Andersen, Nucl. Instr. and Meth. B 14 (1986) 1.
- [30] A. Bouquillon, J.-C. Dran, G. Lagarde, P. Martinetto, B. Moignard, J. Salomon, P. Walter, Nucl. Instr. and Meth. B 188 (2002) 156.
- [31] G. Demortier, A. Adriaens (Eds.), Ion Beam Study of Art and Archaeological Objects, A Contribution by Members of the COST G1 Action, European Commission, EUR 19218, 2000.